International Journal of Engineering, Mathematical and Physical Sciences
ISSN: 2517-9934
Vol:3, No:5, 2009

Numerical Analysis of Electrical Interaction between two Axisymmetric Spheroids

Kuan-Liang Liu, Eric Lee, Jung-Jyh Lee, and Jyh-Ping Hsu

***Abstract*—**The electrical interaction between two axisymmetric spheroidal particles in an electrolyte solution is examined numerically. A Galerkin finite element method combined with a Newton-Raphson iteration scheme is proposed to evaluate the spatial variation in the electrical potential, and the result obtained used to estimate the interaction energy between two particles. We show that if the surface charge density is fixed, the potential gradient is larger at a point, which has a larger curvature, and if surface potential is fixed, surface charge density is proportional to the curvature. Also, if the total interaction energy against closest surface-to-surface curve exhibits a primary maximum, the maximum follows the order (oblate-oblate) > (sphere-sphere) > (oblate-prolate) > (prolate-prolate), and if the curve has a secondary minimum, the absolute value of the minimum follows the same order.

***Keywords*—**interaction energy, interaction force, Poisson-Boltzmann equation, spheroid.

I. Introduction

THE classic DLVO theory [1] assumes that the interaction between two charged lyophobic colloidal particles in an electrolyte solution comprises the van der Waals attractive force and the electrostatic repulsive force. The former is due to the permanent dipole or London dispersion interaction, and the latter arises from the overlapping of the electrical double layers near the particles. To evaluate the electrical interaction between two charged entities, the spatial variation of the electrical potential needs to be known at a prior. According to the Gouy-Chapman's electrical double layer model, at equilibrium it is described by the well-known Poisson-Boltzmann equation [1]. Unfortunately, solving this equation is almost impossible, even for a single charged surface. Often, it is assumed that the electrical potential is low so that the Poisson-Boltzmann equation can be approximated by a linearized expression, which is more readily solvable for simple geometry and idealized surface conditions. Several approximate methods were proposed to solve a linearized Poisson-Boltzmann equation, and to estimate the interaction force and the interaction energy between two charged entities [2]-[10].

In general, a Poisson-Boltzmann equation needs to be solved numerically. Among the possible approaches, the finite difference method has the advantage that it can be coded and implemented easily in common computing facilities such as a personal computer. However, it can become nontrivial if the physical domain involves nonplanar boundary. In the case of two spheres, for instance, bispherical coordinates are necessary, and the physical domain needs to be transformed first to a rectangular computational domain [11]-[13]. For a complicated physical domain, a more sophisticated numerical method such as finite element method is desirable. Chan and Chan [14], for example, used this approach to solve the problem of two identical spheres remained at constant surface potential. James and Williams [15] estimated the distribution of electrical potential for the case of a cylindrical particle and a plane, both are remained at constant surface potential. The former is either parallel or perpendicular to the latter. The mesh sizes were adjusted manually. You and Harvey [16] used a three-dimensional finite element method to solve the Poisson-Boltzmann equation for the case a single bio-macromolecule under the condition of low electrical potential, and the result obtained was compared with that obtained through a finite difference method. Chou Chang and Spostio [17] proposed a self-adaptive finite element method to calculate the electrical potential near a disk-shape particle, taking the anion exclusion volume into account. The same approach was adopted by Bowen and Sharif [18] to evaluate the electrostatic interaction between a charged sphere and a charged pore; the electrical force and free energy were also calculated. Compared with a finite difference method, a finite element method has the merit that it allows using irregular elements, thereby capable of describing, more precisely, a curved or irregular boundary. On the other hand, since the computation usually involves manipulation of large-scale matrices, a finite element method is often complicated and time consuming.

Compared with simple geometries such as infinite plate, long cylinder, and sphere, spheroid is more general in that it is capable of simulating various shapes by adjusting its parameters. This is highly desirable for practical considerations since colloidal particles are found to have various shapes. Reported results for spheroidal surfaces are mainly for limited special cases, for example, thin double layer [19], [20] or low electrical potential [21]-[23]. In the present study, the electrical interaction between two axisymmetric spheroids in an electrolyte solution is discussed. A finite element method coupled with a Newton-Raphson iteration scheme is adopted to solve the Poisson-Boltzmann equation for the system under consideration, and the result obtained is used to evaluate the interaction energy between two particles. Both the electrical and the van der Waals interaction energies are estimated.

K. .L. Liu is with the department of chemical engineering, National Taiwan University, Taipei Tiwan 10617 (corresponding author to provide phone: 886-2-23637448; fax: 886-2-23623040; e-mail: f96524027@ntu.edu.tw).

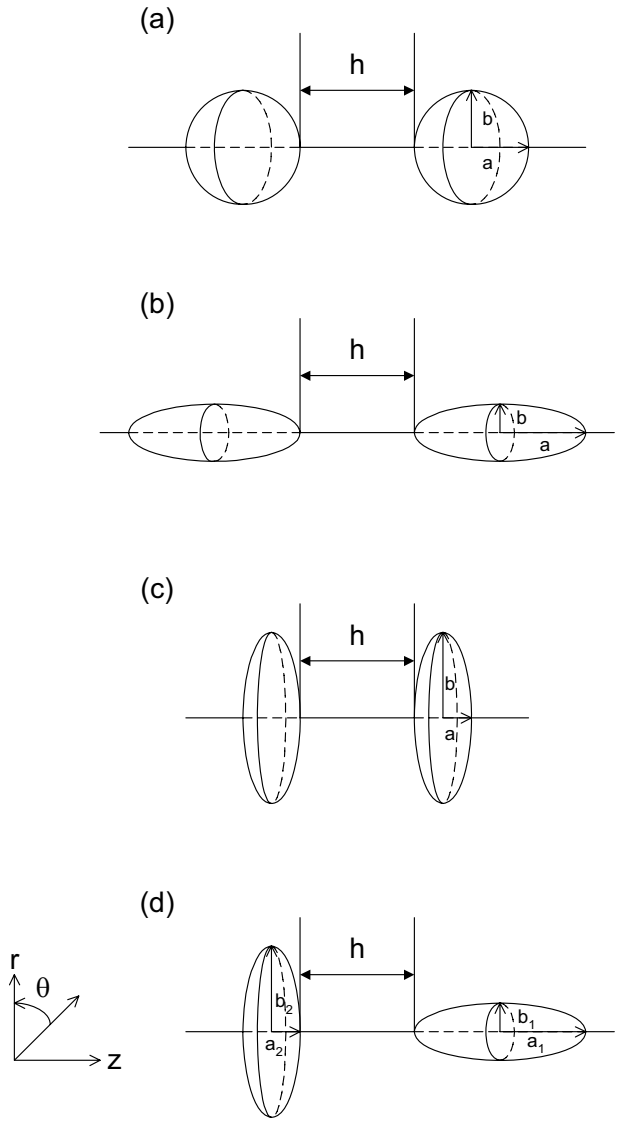

Fig.1. Schematic representation of the system under consideration. h is the scaledclosest surface-to-surface distance between two particles, a and b are the semi-major and semi-minor axis of a particle, respectively. (a): sphere-sphere,(b) prolate-prolate, (c) oblate-oblate, (d) oblate (1)-prolate (2).

II. Theory

We consider two axisymmetric spheroidal particles in an electrolyte solution. By referring to Fig.1, let h be the dimensionless closest surface-to-surface distance between them, scaled by ℓ =(a+b)/2, a and b being respectively the semi-major and semi-minor axes of a particle. The special case with a=b leads to two spheres. For 1:1 electrolytes, the spatial variation of electrical potential at equilibrium, ϕ, is described by [1]

$$\nabla^2\phi = \frac{2en_b}{\varepsilon_0\varepsilon_r}\sinh\left(\frac{e\phi}{kT}\right) \tag{1}$$

where ∇^2 denotes the Laplace operator, ε_0 and ε_r are respectively the permittivity of a vacuum and the relative permittivity, n_b is the bulk electrolyte concentration, k and T are respectively the Boltzmann constant and the absolute temperature, and e is the elementary charge. If both the surfaces of the particles are maintained at constant charge density, then the boundary conditions associated with (1) are

$$-\varepsilon_0\varepsilon_r\frac{\partial\phi}{\partial n^*} = q^*_{s1} \text{ on } S_1 \tag{2a}$$

$$-\varepsilon_0\varepsilon_r\frac{\partial\phi}{\partial n^*} = q^*_{s2} \text{ on } S_2 \tag{2b}$$

where S_1 and S_2 denote the surfaces of particles 1 and 2 respectively, q^*_{s1} and q^*_{s2} are respectively the surface charge densities of particles 1 and 2, and n* is the outward normal of a surface. Here we assume that the relative permittivity of the solid phase is much smaller than that of the liquid phase, as is usually satisfied for an aqueous dispersion. Similarly, if both S_1 and S_2 are maintained at constant potential, then the boundary conditions associated with (1) become

$$\phi = \phi_{s1} \text{ on } S_1 \tag{3a}$$

$$\phi = \phi_{s2} \text{ on } S_2 \tag{3b}$$

where ϕ_{s1} and ϕ_{s2} are the surface potentials of particles 1 and 2 respectively.

The cylindrical coordinates (r^*,θ,Z^*) are adopted in the subsequent analysis, and the particles are placed such that they are symmetric about Z* axis. For a simpler treatment, equation (1) is rewritten in the following scaled form:

$$\frac{\partial^2\psi}{\partial z^2} + \frac{1}{r}\frac{\partial}{\partial r}\left(r\frac{\partial\psi}{\partial r}\right) = (\kappa\ell)^2\sinh\psi \tag{4}$$

where $z = z^*/\ell$, $r = r^*/\ell$, and $\psi = e\phi/kT$. The scaled coordinates (r,θ,Z) are illustrated in Fig.1. The characteristic length ℓ is the average of the semi-major and semi-minor axes of a particle, and the reciprocal Debye length κ is defined by

$$\kappa = \sqrt{\frac{2e^2 n_b}{\varepsilon_0 \varepsilon_r kT}} \tag{5}$$

The corresponding scaled boundary conditions become

$$-\frac{\partial \psi}{\partial n} = q_{s1} \text{ on } S_1 \tag{6a}$$

$$-\frac{\partial \psi}{\partial n} = q_{s2} \text{ on } S_2 \tag{6b}$$

for constant surface charge density, or

$$\psi = \psi_{s1} \text{ at } S_1 \tag{7a}$$

$$\psi = \psi_{s1} \text{ at } S_2 \tag{7b}$$

for constant surface potential, where $q_{s1} = q_{s1}^{*} \varepsilon_0 \varepsilon_r kT/e\ell$, $n=n^*/\ell$, $q_{s2} = q_{s2}^{*} \varepsilon_0 \varepsilon_r kT/e\ell$, $\psi_{s1} = (\phi_{s1} kT/e)$, and $\psi_{s2} = (\phi_{s2} kT/e)$.

The total interaction energy between two particles, V_T, is the sum of the electrical energy, V_R, and the van der Waals energy, V_{VDW}, that is

$$V_T = V_{VDW} + V_R \tag{8}$$

The dimensionless electrical repulsive force between two particles, f, scaled by $\varepsilon_0 \varepsilon_r (kT/e)^2$, can be calculated by [3]

$$f(h) = \frac{1}{\varepsilon_0 \varepsilon_r (kT/e)^2} \int_{\Xi} [\Delta\pi + \frac{\varepsilon_0 \varepsilon_r E^2}{2}) \vec{n} - \varepsilon_0 \varepsilon_r (\vec{E} \bullet \vec{n}) \vec{E}] dE \tag{9}$$

where $\Delta\pi$ is the osmotic pressure, $\vec{n}$ is the outward normal vector, $\vec{E}$ is the electric field vector with strength E, and Ξ represents a plane between the particles which is perpendicular to Z axis. Note that Ξ needs not to be located at the center plane between two particles. The osmotic pressure can be evaluated by

$$\Delta\pi = \varepsilon_0 \varepsilon_r \left(\frac{kT}{e}\right)^2 \kappa^2 [\cosh(\psi) - 1] \tag{10}$$

(5)

For the present axisymmetric problem, substituting this expression into (9) leads to

$$f(h) = \pi \int_0^{\infty} \left[2(\kappa\ell)^2 (\cosh\psi - 1) + \left(\frac{\partial \psi}{\partial r}\right)^2 - \left(\frac{\partial \psi}{\partial z}\right)^2 \right] r dr \tag{11}$$

(6a)

The electrical interaction energy between two particles can be evaluated by [24]

(6b)

$$V_R = \varepsilon_0 \varepsilon_r \ell \left(\frac{kT}{e}\right)^2 \int_h^{\infty} f(h') dh' \tag{12}$$

(7a)

(7b)

The van der Waals interaction energy between two particles can be evaluated by [1]

$$V_{VDW} = -\frac{A_{132}}{\pi^2} \int_{V_1} \int_{V_2} \frac{1}{r^6} dV_2 dV_1 \tag{13}$$

where V_1 and V_2 denote respectively the volumes of particles 1 and 2, and A_{132} is the Hamaker constant. For the present axisymmetric case, it can be shown that equation (13) becomes

(8)

$$V_{VDW} = -A_{132} \int_{a_2}^{b_2} \int_{a_1}^{b_1} \frac{1}{4d^4} \left\{ (\beta^2 + \gamma^2) - \frac{(\beta^2 - \gamma^2)^2 + d^2(\beta^2 + \gamma^2)}{\sqrt{[(\beta+\gamma)^2 + d^2][(\beta-\gamma)^2 + d^2]}} \right\} dL_1 dL_2 \tag{14}$$

where

$$d = h\ell + a_1 + a_2 + L_1 + L_2 \tag{14a}$$

$$\beta = b_1 \sqrt{1 - (L_1/a_1)^2} \tag{14b}$$

$$\gamma = b_2 \sqrt{1 - (L_2/a_2)^2} \tag{14c}$$

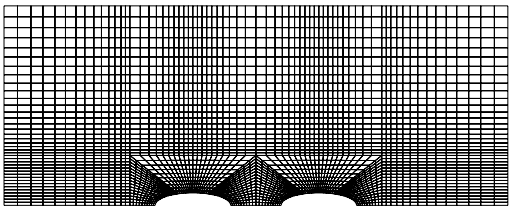

(a)

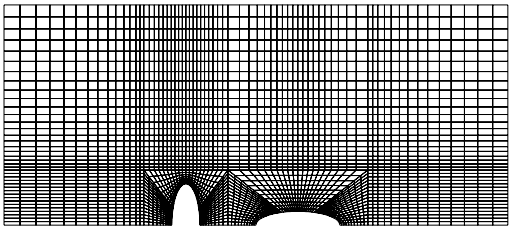

(b)

Fig.2. Examples for the finite element meshes used in the numerical scheme.(a): prolate-prolate, (b): oblate-prolate.

III. Numerical Method

The Galerkin finite element method coupled with a Newton-Raphson iteration scheme is used to solve (4), the result obtained is substituted into (11) to evaluate f(h), and equation (12) is then used to calculate V_R. The solution to the linearized version of (4) is used as the initial guess for the Newton-Raphson iteration scheme. The frontal method proposed by Iron [25] and Hood [26] is adopted to improve the computational efficiency. A 9-node quadrilateral isoparametric element is adopted in the finite element method. Typical meshes used are illustrated in Figs. 2(a) and 2(b). Both the conditions of constant surface potential and constant surface charge density are considered. The estimation of the van der Waals interaction energy is based on a 96×96 Gauss quadrature. A Digital DEC3000 model 700AXP work station is used to perform all the necessary calculations. The convergence of the solution is checked with mesh refinement. With fewer or more grid points, the deviations of the solutions are less than 1%. We thus conclude that the solution obtained with the current mesh is the convergent solution to the original governing differential equations.

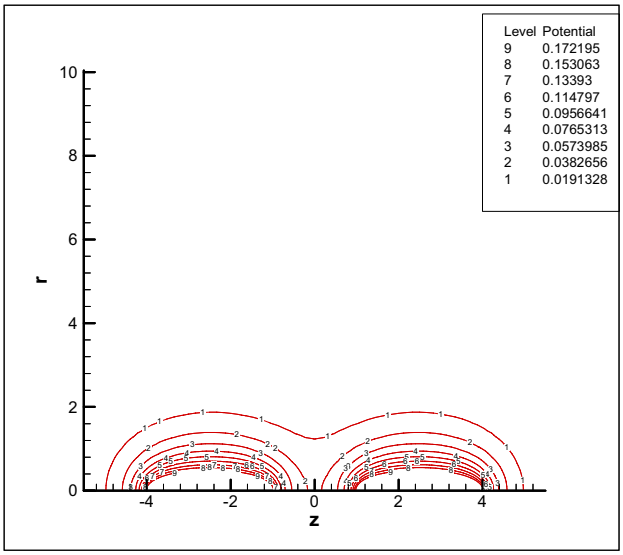

(a)

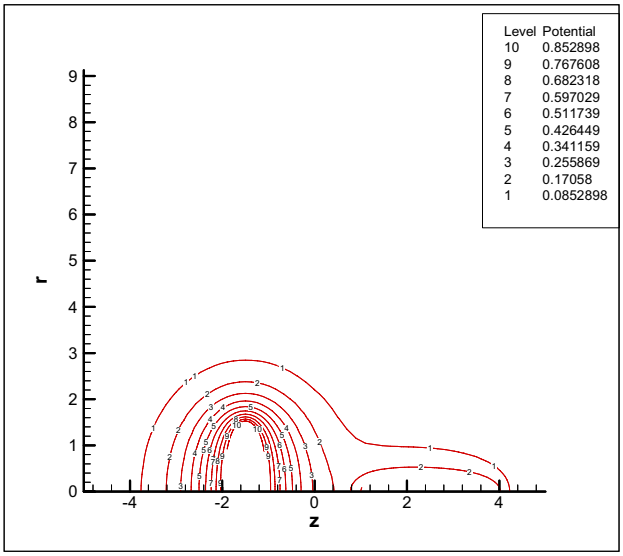

(b)

Fig.3. Contours of electrical potential distribution for the case of prolate-prolate, (a),and oblate-prolate, (b), at constant surface charge density. Parameters used:$q_{s1}=q_{s2}=1$, $\kappa\ell=1.0$, and h=2.0.

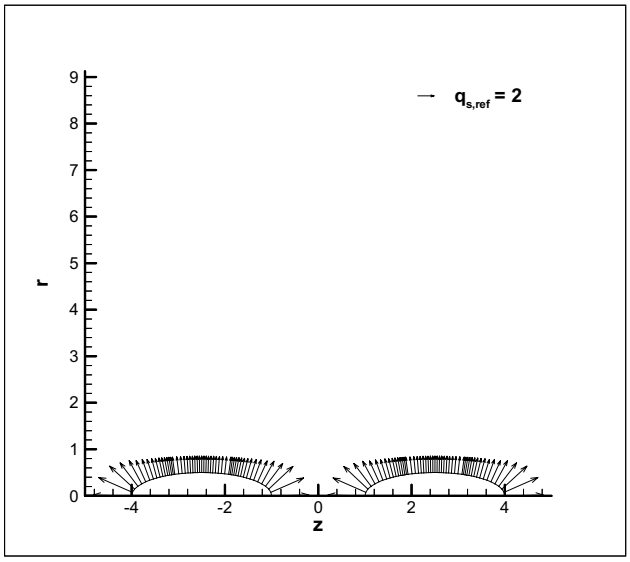

(a)

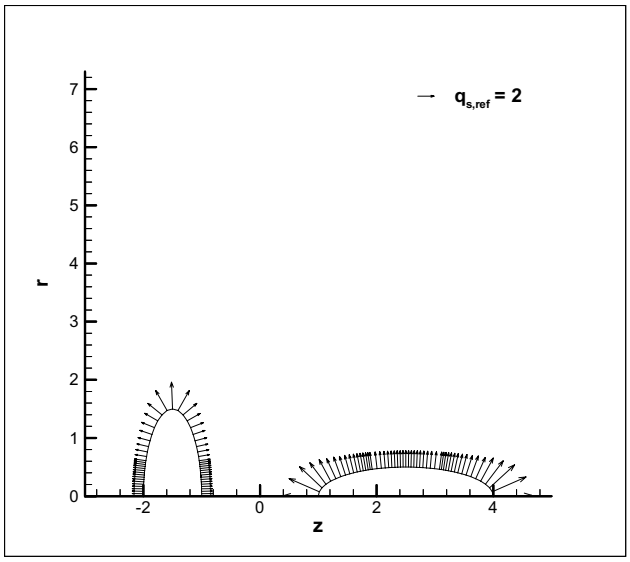

(b)

Fig.4. Variation of surface charge density for the case of prolate-prolate, (a),and oblate-prolate, (b), at constant surface potential. Parameter used: $\Psi_{S1} = \Psi_{S2} = 1$, $\kappa\ell = 1.0$, and h=2.0.

IV. Resuls and Disccusion

We consider the four cases shown in Fig.1 in the numerical calculations: sphere-sphere, prolate-prolate, oblate-oblate, and oblate (1)-prolate (2). The interaction between two spheres is a special case of the present study which can be recovered from the spheroids by letting $a_i=b_i$. For illustration, we assume that the lengths of the major and minor axes of a particle are 150 nm and 50 nm, respectively, and the radius of a spherical particle is 100 nm. Two typical spatial variations of the electrical potential for prolate-prolate and oblate-prolate are illustrated respectively in Fig.3, and the corresponding variations in the surface charge density are shown in Fig.4. As can be seen from Fig.3, if the surface charge density is fixed, the potential gradient is larger at a point, which has a larger curvature. Figure 4 reveals that if surface potential is fixed, surface charge density is proportional to the curvature.

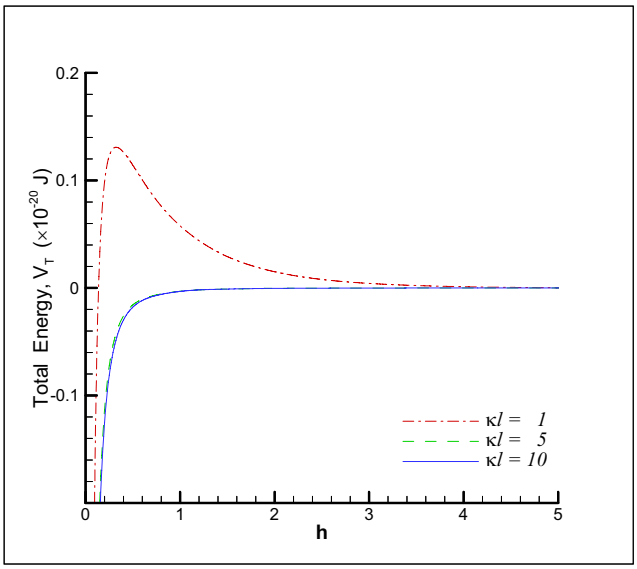

Fig.5. Variation of total interaction energy, V_T, between two prolates at constantsurface charge density as a function of the scaled closest surface-to-surfacedistance, h, at various $\kappa\ell$ for the case $q_{s1}=q_{s2}=1$ and $A_{132}=10^{-19}$ J.

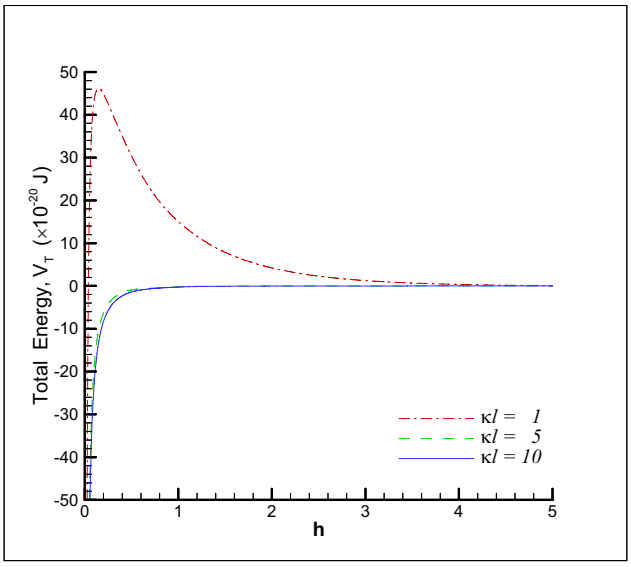

Fig.6. Variation of total interaction energy, V_T, between two oblates at constantsurface charge density as a function of the scaled closest surface-to-surfacedistance, h, at various $\kappa\ell$ for the case $q_{s1}=q_{s2}=1$ and $A_{132}=10^{-19}$ J.

Figures 5 through 8 present the variations of total interaction energy between two particles, V_T, as a function of the scaled closest surface-to-surface distance between them, h, at various $\kappa\ell$ for the case of constant surface charge density. These figures suggest that, all the four cases examined V_T exhibit a primary maximum, and the maximal V_T follows the order (oblate-oblate) > (sphere-sphere) > (oblate-prolate) > (prolate-prolate). The values of h at which the maximum occur, however, are different for each case.

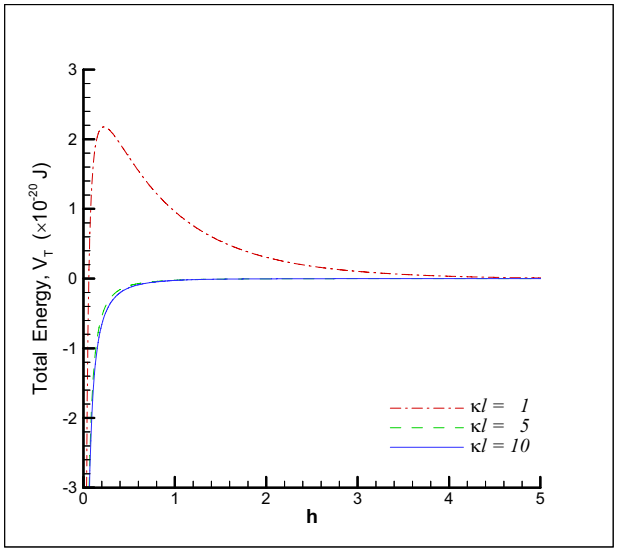

Fig.7. Variation of total interaction energy, V_T, between on oblate and a prolate atconstant surface charge density as a function of the scaled closest surface-to-surface distance, h, at various $\kappa\ell$ for the case $q_{s1}=q_{s2}=1$ and $A_{132}=10^{-19}$ J.

The variations of total interaction energy between two particles, V_T, as a function of the scaled closest surface-to-surface distance between them, h, at various $\kappa\ell$ for the case of constant surface potential are shown in Figs.9 through 12. The general trends of the V_T against h curves are similar to those for the case of constant surface charge density shown in Figs.5 through 8 except that if $\kappa\ell$ is sufficiently large, a negative second minimum is observed in each case. The absolute value of the minimum follows the same order as that of the primary maximum.

The numerical scheme proposed in the present study can be modified without too much difficulty to the case of two arbitrary axisymmetric entities. For the case of z_a:z_b electrolyte, z_a and z_b being the valences of cations and anions respectively, equation (4) becomes

$$\frac{\partial^2\psi}{\partial z^2}+\frac{1}{r}\frac{\partial}{\partial r}\left(r\frac{\partial\psi}{\partial r}\right)=(\kappa\ell)^2\frac{\exp(b\psi)-\exp(-a\psi)}{z_a+z_b} \quad (15)$$

with

$$\kappa=\sqrt{\frac{e^2\left(z_a^2n_+^0+z_b^2n_-^0\right)}{\varepsilon_0\varepsilon_r kT}} \quad (16)$$

where n_+^0 and n_-^0 denote respectively the bulk number concentrations of cations and anions. The numerical procedure remains the same as that employed in the case of 1:1 electrolyte.

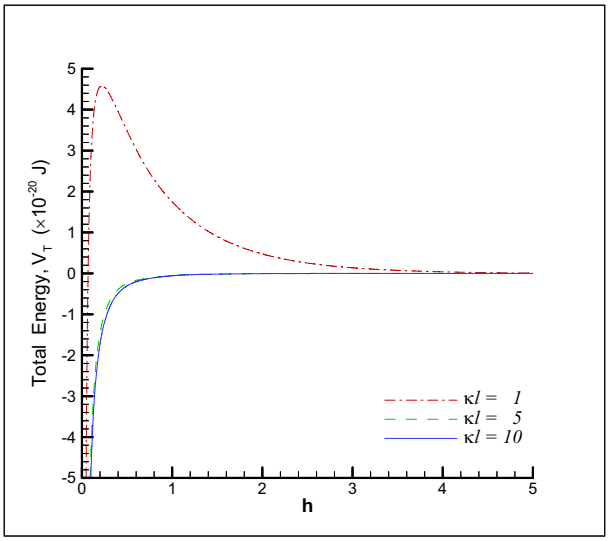

Fig.8. Variation of total interaction energy, V_T, between two spheres at constantsurface charge density as a function of the scaled closest surface-to-surfacedistance, h, at various $\kappa\ell$ for the case $q_{s1}=q_{s2}=1$ and $A_{132}=10^{-19}$ J.

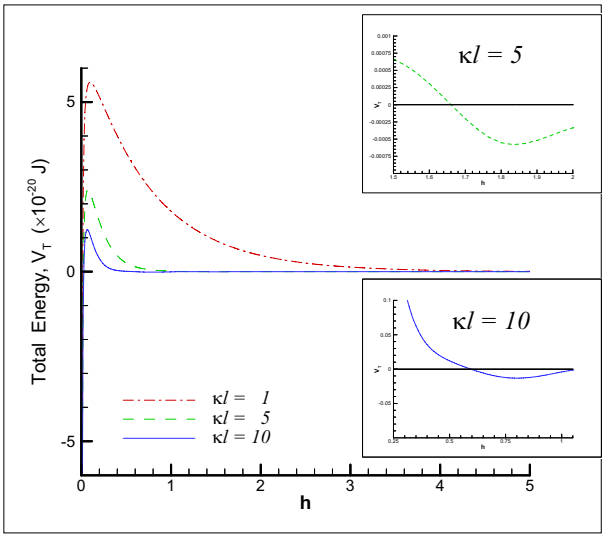

Fig.9. Variation of total interaction energy, V_T, between two prolates at constantsurface potential as a function of the scaled closest surface-to-surface distance, h, at various $\kappa\ell$ for the case $\Psi_{s1}=\Psi_{s2}=1$ and $A_{132}=10^{-19}$ J.

The computing time of the present finite element method increases with $\kappa\ell$. This is because that, for fixed particle size, if the concentration of electrolyte is high, the double layer near a particle becomes thin. In this case the finite element meshes need to be allocated in a small interval in space, or, equivalently, the number of meshes needs to be increased for a fixed interval to achieve a desired degree of accuracy. Since the number of meshes is limited by the available computing facility, the alternative is to increase the number of iterations, and the computing time increases accordingly. The present numerical scheme becomes inefficient if $\kappa\ell$ exceeds about 20. Note that, however, if $\kappa\ell$ is sufficiently large, the particles can be treated as planar ones, and the problem under consideration can be simplified significantly.

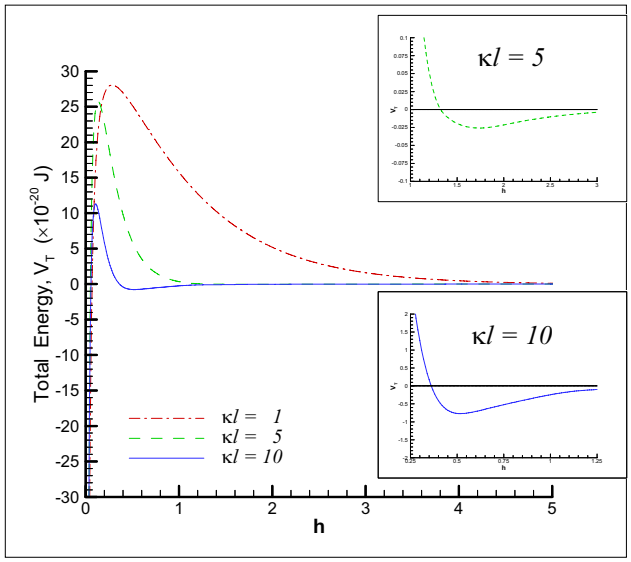

Fig.10. Variation of total interaction energy, V_T, between two oblates at constantsurface potential as a function of the scaled closest surface-to-surfacedistance, h, at various $\kappa\ell$ for the case $\Psi_{s1} = \Psi_{s2} = 1$ and $A_{132} = 10^{-19}$ J.

V. Conclusion

In summary, the electrical interaction between two axisymmetric spheroids is examined numerically. Compared with simple geometry such as spheres, spheroids are capable of simulating a wide class of particles, and can be used to include the effect of the variation of curvature over particle surface. The former is highly desirable in practice since colloidal particles may assume various shapes, and the latter is significant when the relative orientation between two particles needs to be taken into account. Here, we examine the possibility of solving the problem involving two spheroids through a finite element method. The efficiency of the algorithm proposed here may be improved with additional numerical skills. Nevertheless, it provides a way of investigating the electrical interaction between two axisymmetric particles in an electrolyte solution.

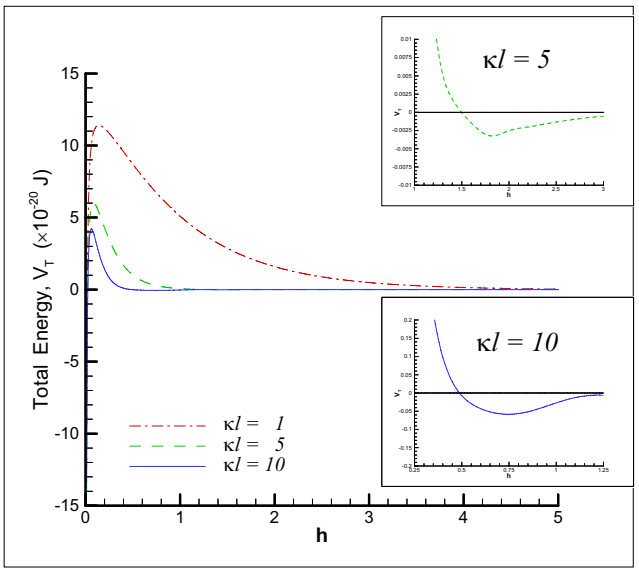

Fig.11. Variation of total interaction energy, V_T, between on oblate and a prolate atconstant surface potential as a function of the scaled closest surface-to-surface distance, h, at various $\kappa\ell$ for the case $\Psi_{s1} = \Psi_{s2} = 1$ and $A_{132} = 10^{-19}$ J.

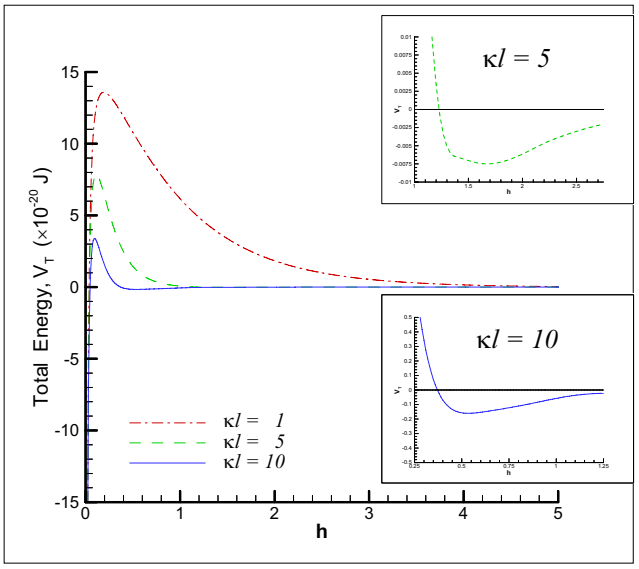

Fig.12. Variation of total interaction energy, V_T, between two spheres at constantsurface potential as a function of the scaled closest surface-to-surfacedistance, h, at various $\kappa\ell$ for the case $\Psi_{s1} = \Psi_{s2} = 1$ and $A_{132} = 10^{-19}$ J.

ACKNOWLEDGMENT

This work is supported by the National Science Council of the Republic of China.

REFERENCES

[1] R.J. Hunter, *Foundations of Colloid Science*, Vol. I, Oxford University Press, London, 1992.
[2] B.V. Derjaguin and L.D. Landau, *Acta Phys.-Chim.* USSR, 14 (1941) 633.
[3] G.M. Bell, S. Levine, and L.N. McCartney, *J. Colloid Interface Sci.*, 33 (1970) 335.
[4] H. Ohshima, D.Y.C. Chan, T.W. Healy and L.R. White, *J. Colloid Interface Sci.*, 92 (1983) 232.
[5] S.L. Carnie and D.Y.C. Chan, *J. Colloid Interface Sci.*, 155 (1993) 297.
[6] J.E. Sader, S.L. Carnie and D.Y.C. Chan, *J. Colloid Interface Sci.*, 171 (1995) 46.
[7] C.E. McNamee, Y. Tsujii, H. Ohshima, et al., *Langmuir*, 20 (2004) 1953
[8] H. Ohshima, *Lngmuir*, 23 (2007) IX.
[9] V Krautler and P.H. Hunenberger, *Mol. Simul*., 34 (2008) 491.
[10] H. Ohshima, *J. Colloid Interface Sci.*, 328 (2008) 3.
[11] N.E. Hoskins and S. Levine, *Philos. Trans. R. Soc. London A* 248, **(**1956) 433.
[12] J.E. Ledbetter, T.L. Croxton and D.A. McQuarrie, *Can. J. Chem.*, 59 (1981) 1860.
[13] S.L. Carnie, D.Y.C. Chan and J. Stankovich, *J. Colloid Interface Sci.*, 165 (1994) 116.
[14] B.K.C. Chan and D.Y.C. Chan, *J. Colloid Interface Sci.*, 92 (1983) 281.
[15] A.E. James and D.J.A. Williams, *J. Colloid Interface Sci.*, 107 (1985) 44.
[16] Y.J. You and C. Harvey, *J. Comput. Chem.*, 14 (1993) 484.
[17] F.R. Chou Chang and G. Sposito, *J. Colloid Interface Sci.*, 163 (1994) 19.
[18] W.R. Bowen and A.O. Sharif, *J. Colloid Interface Sci.*, 187 (1997) 363.
[19] B.T. Liu and J.P. Hsu, *J. Chem. Phys.*, 128 (2008) 104509.
[20] J.J. Feng and W.Y. Wu, *J. Fluid Mech.*, 264 (1994) 41.
[21] J.P. Hsu and B.T. Liu, *J. Colloid Interface Sci.*, 178 (1996) 785.
[22] J.P. Hsu, C.C. Kuo and M.H. Ku, *Electrophoresis*, 29 (2008) 348.
[23] J.P. Hsu, C.Y. Chen and D.J. Lee, et al, *J. Colloid Interface Sci.*, 325 (2008) 516.
[24] Y.C. Kuo and J.P. Hsu, *J. Colloid Interface Sci.*, 156 (1993) 250.
[25] B.M. Irons, Int. *J. Num. Methods Eng.*, 2 (1970) 5.
[26] P. Hood, Int. *J. Num. Methods Eng.*, 10 (1976) 379.